J Mater Sci: Mater Med (2011) 22:2659–2672
DOI 10.1007/s10856-011-4453-x

Effect of phosphate-based glass fibre surface properties on thermally produced poly(lactic acid) matrix composites

Maziar Shah Mohammadi · Ifty Ahmed · Naser Muja · Christopher D. Rudd · Martin N. Bureau · Showan N. Nazhat

Received: 2 September 2011 / Accepted: 29 September 2011 / Published online: 16 October 2011

Abstract Incorporation of soluble bioactive glass fibres into biodegradable polymers is an interesting approach for bone repair and regeneration. However, the glass composition and its surface properties significantly affect the nature of the fibre-matrix interface and composite properties. Herein, the effect of Si and Fe on the surface properties of calcium containing phosphate based glasses (PGs) in the system ($50P_2O_5$-40CaO-(10-x)SiO_2-xFe_2O_3, where $x = 0$, 5 and 10 mol.%) were investigated. Contact angle measurements revealed a higher surface energy, and surface polarity as well as increased hydrophilicity for Si doped PG which may account for the presence of surface hydroxyl groups. Two PG formulations, $50P_2O_5$-40CaO-$10Fe_2O_3$ (Fe10) and $50P_2O_5$-40CaO-$5Fe_2O_3$-$5SiO_2$ (Fe5Si5), were melt drawn into fibres and randomly incorporated into poly(lactic acid) (PLA) produced by melt processing. The ageing in deionised water (DW), mechanical property changes in phosphate buffered saline (PBS) and cytocompatibility properties of these composites were investigated. In contrast to Fe10 and as a consequence of the higher surface energy and polarity of Fe5Si5, its incorporation into PLA led to increased inorganic/organic interaction indicated by a reduction in the carbonyl group of the matrix. PLA chain scission was confirmed by a greater reduction in its molecular weight in PLA-Fe5Si5 composites. In DW, the dissolution rate of PLA-Fe5Si5 was significantly higher than that of PLA-Fe10. Dissolution of the glass fibres resulted in the formation of channels within the matrix. Initial flexural strength was significantly increased through PGF incorporation. After PBS ageing, the reduction in mechanical properties was greater for PLA-Fe5Si5 compared to PLA-Fe10. MC3T3-E1 preosteoblasts seeded onto PG discs, PLA and PLA-PGF composites were evaluated for up to 7 days indicating that the materials were generally cytocompatible. In addition, cell alignment along the PGF orientation was observed showing cell preference towards PGF.

Electronic supplementary material The online version of this article (doi:10.1007/s10856-011-4453-x) contains supplementary material, which is available to authorized users.

M. Shah Mohammadi · N. Muja · M. N. Bureau · S. N. Nazhat (✉)
Department of Mining and Materials Engineering, McGill University, Rm 2090, Wong Building, 3610 University Street, Montreal, QC H3A 2B2, Canada
e-mail: showan.nazhat@mcgill.ca

I. Ahmed · C. D. Rudd
Division of Mechanics, Materials and Structures, University Park Campus, University of Nottingham, Nottingham NG7 2RD, UK

M. N. Bureau
Industrial Materials Institute, National Research Council Canada, Boucherville, QC J4B 6Y4, Canada

1 Introduction

Composites of biodegradable polymers and bioactive ceramics have been developed for bone repair and regeneration [1–6]. The incorporation of inorganic fillers such as silicate based bioactive glasses (e.g. Bioglass®) and hydroxyapatite into degradable polymers (e.g. poly(lactic acid) (PLA), poly(glycolic acid) (PGA), their copolymers (PLGA) and polycaprolactone (PCL) [7, 8]) has been shown to enhance the Young's modulus, flexural strength and osteoconductivity of the composites [9–11]. Also, in an effort to tailor the degradation properties of composites, phosphate-based glasses (PGs) have emerged as inorganic fillers [12, 13]. PGs provide several advantages: (i) their

solubility can be predicted and easily controlled through their composition [14–16]; (ii) their polymeric nature allows for some formulations to be drawn into fibres [17]; and (iii) the high surface area to volume ratio of PG fibres (PGFs) can significantly affect their degradation and the release of potentially therapeutic ions, which can influence the biological properties of the composites. Thus, by doping calcium-PGs with various amounts of modifying oxides, the solubility and ion release rate can be controlled for bone regeneration approaches, as well as tailoring the composite mechanical properties.

Glass network modifying oxides not only change the bulk properties of PGs, but also their surface properties such as surface energy and hydrophilicity. These properties significantly affect the hydrolysis of the glass. Since P_2O_5 is chemically unstable due to easily hydrolysable P–O-P bonds, the addition of glass modifying metal oxides, such as Fe_2O_3, increases the PG stability by creating P–O-Fe bonds that are generally less hydrolysable. Abou Neel et al. [18] investigated the synergy between composition and surface properties of PGs and its effect on the degradation and ion release of iron containing PGFs and showed that, in the P_2O_5-CaO-Na_2O-Fe_2O_3 system, the polar interactions occurring on the glass surfaces diminished with increasing Fe_2O_3 content. There was a reduction in the overall surface energy with an increase in Fe_2O_3 content which was attributed to the decrease in polar or acid/base component. The hydrophilicity and surface energy of the PG could also influence its interfacial interaction with the polymer matrix. It has previously been shown that thermally produced composites of PCL filled with particulates of Si doped PG resulted in a reduction of PCL matrix molecular weight as a consequence of a reaction between the glass particulates and the ester bonds, which created carboxylate by-products [19]. Matrix degradation increased with increasing Si content. In terms of PG degradation, it has been shown that the addition of Si disrupts the phosphate network leading to a higher dissolution rate of the glass in aqueous environments [14].

Blaker et al. [20] also demonstrated that the inclusion of Bioglass® particles caused a reaction at the filler-poly (D, L-lactide) interface when processed at elevated temperatures. This in turn degraded the polymer matrix leading to a reduction in the mechanical properties of the composite. Therefore, along with the composition and volume fraction of the filler and its solubility, processing conditions are also critical for composite properties [20]. Bioglass® has a high surface energy [21] and creates Si–OH groups on the surface by absorbing water which will subsequently hydrolyse the ester bond causing matrix chain-scission [20].

Therefore, since the surface properties of glasses can have a considerable effect on the filler/matrix interface and composite properties, the aim of this study was to investigate the effect of Fe and Si doped PG fibres on PLA matrix composite properties, when thermally produced. The surface energy of PGs of the system $50P_2O_5$-40CaO-(10-x)SiO_2-xFe_2O_3, where $x = 0$, 5 and 10 mol.% was measured. The degradation and morphological changes of properties of PLA-PGF were investigated in deionised water for up to 56 days, the mechanical properties of the composites were investigated initially and when aged in phosphate buffered saline (PBS) for up to 28 days. In addition, the cytocompatibility of the glasses and composites was assessed using MC3T3-E1 preosteoblasts to investigate their potential application in bone repair and regeneration.

2 Materials and methods

2.1 Phosphate glass (PG) production

Three melt derived PG compositions (Table 1) were prepared using P_2O_5, $CaHPO_4$, Fe_2O_3, and SiO_2 (Sigma Aldrich) as starting materials. The precursors were dry blended, poured into a Pt/10%Rh crucible (Birmingham Metal Company), and heated to 400°C in order to remove moisture. The crucible was then transferred to a second furnace and melted at 1150°C for 90 min. The molten glass was then cast into a cylindrical shape mould (10 mm in diameter), annealed at 350°C for 1 h to remove any residual stresses and cut into discs, or poured onto a steel plate and cooled to room temperature to make the bulk glass.

A specialist in house fibre-drawing rig was used to produce glass fibres utilising a melt drawn technique from the following ternary and quaternary formulations; $50P_2O_5$-40CaO-10Fe_2O_3 (Fe10) and $50P_2O_5$-40CaO-5Fe_2O_3-5SiO_2 (Fe5Si5). PGFs were guided onto a rotating drum at 1600 rpm to produce fibres in the range of 10–20 μm in diameter. The fibres were removed from the drum and annealed by heating up to 200°C at 20°C/min, then heating to 505°C at 1°C/min and holding for 90 min, cooling to 300°C at 0.25°C/min and finally cooling to room temperature at 1°C/min. Once annealed overnight, the fibres were cut to lengths of 10 mm to prepare the random fibre mats.

Table 1 Glass compositions and coding

Glass code	Components (mol.%)			
	P_2O_5	CaO	SiO_2	Fe_2O_3
Si10	50	40	10	–
Fe5Si5	50	40	5	5
Fe10	50	40	0	10

2.2 PLA-PGF composite production

PGFs (3 g of 10 mm length) were dispersed into a 4 l solution of distilled water and Cellosize (Univar Ltd) for 10 min. The fibre-cellulose solution was then poured into a second container consisting of a straining mesh. After ensuring that all fibre aggregates were evenly dispersed, the mesh strainer was extracted from the solution. The resulting random fibre mats were then rinsed with distilled water to remove any residual binder and vacuum-dried at 50°C overnight. PLA pellets (5 g, Resin 3051-D, Natureworks®, molecular weight ~ 91,000 confirmed by GPC) were heated to 210°C and pressed at 3 bar for 30 s (J.R. Dare Ltd., heated press) to produce PLA films of ~ 0.2 mm thickness. The films were cooled under pressure to room temperature using a cold press (Daniels Upstroke Press). Six dried random fibre mats were placed in an alternating sequence with seven PLA films into a metal shim, shielded by two poly(tetrafluoroethylene) sheets, and placed in the hot press (J.R. Dare Ltd), set at 210°C. This stack of PLA films and random fibre mats were then heated at 210°C for 15 min followed by pressing for 15 min at 38 bar, and finally cooled in another press (Daniels Upstroke) for a further 15 min, at 38 bar. Using this procedure, PLA-PGF composites with ~ 18 vol.% PGF were produced (see Table 2). The volume fractions of the composites were calculated using the matrix burn-off method (ASTM D2584-94 [22]). A PLA plaque was also produced following the same film stacking technique.

2.3 Bulk and surface characterisation of PGs

2.3.1 X-ray diffraction of the crystallised PG

X-ray diffraction (XRD) was used to identify the phases present within the crystalline state of the glasses. PGs were crystallised for 3 h at 775°C. XRD was conducted using a Bruker Diffractometer (Bruker AXS Inc.) in flat plate geometry from $2\Theta = 6$ to 86°, with Ni-filtered Cu k_{α} radiation, and using a Philips Diffractometer (PW1710) from $2\Theta = 5$ to 100° with a step size of 0.02 and a count time of 0.1 s. The patterns were analysed using the EVA software package.

Table 2 Composite compositions and coding

Composite code	Components (vol.%)		
	PLA	Fe10	Fe5Si5
PLA	100	0	0
PLA-Fe10	82	18	0
PLA-Fe5Si5	82	00	18

2.3.2 Wettability and surface free energy of the PG

Surface properties of PGs were measured through their wettability and surface free energy. Glass discs from each composition were abraded against silicon carbide paper (1200/4000, Struers) using ethanol as the lubricant. Prior to testing, the specimens were ultrasonicated in ethanol for 20 min and allowed to dry. The static contact angle was measured with a contact angle system OCA (Future Digital Scientific) and ultrapure water and diiodomethane (DII) were used to represent polar and non-polar characteristics, respectively. Droplets (5 µl) were placed on the glass surface via a syringe and the drop profile was recorded for 10 s. The contact angle was calculated after 2 s from the time the droplet was in contact with the surface. The measurements were carried out on triplicate samples. The surface free energy was calculated using the OWRK (Owens, Wendt, Rable and Kaelble) method via SCA20 software.

2.4 Structural characterisation of the PLA-PGF composites

Attenuated total reflectance-Fourier transform infrared spectroscopy (ATR-FTIR) was used to investigate the structural changes in the PLA matrix due to its potential interactions with PGF after thermal processing. Spectra were obtained from neat PLA and as processed composites using a PerkinElmer 400 FTIR. This study was conducted in the 600–3500 cm^{-1} range with a 4 cm^{-1} resolution, and number of scans of 32. All the spectra were normalised to the peak at 1453 cm^{-1}.

Gel permeation chromatography (GPC, Water Breeze) was used to investigate the molecular weight (M_w) of PLA after composite fabrication. The GPC was equipped with both ultraviolet (UV 2487) and differential refractive index (RI 2410) detectors and three Water Styragel HR columns (HR1 with molecular weight measurement in the range of 100–5,000 g/mol, HR2 with molecular weight measurement range of 500–20,000 g/mol, and HR4 with molecular weight measurement range of 5,000–600,000 g/mol and a guard column. The columns were kept at 40°C. Tetrahydrofuran (THF) flowing at a rate of 0.3 ml/min was used as the mobile phase. Each sample dissolved in THF was filtered through a 0.2 µm syringe filter (Anotop25, Fisher) to remove PGF prior to injection into the module.

2.5 Ageing of composites

2.5.1 Ion release and weight loss in deionised water

PLA-PGF composites were aged in deionised water (DW) for up to 56 days by placing specimens ($n = 3$, $10 \times 10 \times 1.6$ mm^3) into vials containing 25 ml of ultra-pure deionised water (18.2 MΩ cm resistivity) and incubating at 37°C. Ion

release, weight loss, and pH of the ageing environment were measured at 14 different time points (0, 2, 4, 8, 24, 48, 96, 168, 336, 504, 672, 840, 1008, and 1344 h).

Anions and cations released via composite degradation were measured using ion chromatography (IC) and atomic absorption (AA), respectively. IC (Dionex, DX-100 Ion Chromatograph) was used in order to measure phosphate anion (PO_4^{3-}) release. An Ionpac AS14 anion exchange column was used to elute the phosphates. An eluent of 3.5 mM Na_2CO_3/ 0.1 mM $NaHCO_3$ was used with a flow rate of 0.1 ml/min with sample run time of 15 min. Sodium phosphate tribasic (Na_3PO_4) (Sigma, Canada) was used to prepare standard solutions. A 1000 ppm working solution was prepared from which serially diluted 10, 20, and 50 ppm standard solutions were obtained. AA (VARIAN AA240FS) was used to investigate the release of Ca^{2+}, Fe^{3+}, and Si^{4+} cations. The instrument was calibrated using certified AA standard solutions.

The weight change of the composites was investigated by removing the specimens from DW, blot drying, weighing and replacing in fresh deionised water. Weight loss was measured in terms of percentage of original weight. The final dry weight at day 56 was measured by first incubating the specimens for 6 days at 37°C until an equilibrium weight was reached.

The pH of the deionised water was also measured using a pH meter (Accumet Excel 20, Fisher) at each time point.

2.5.2 *Morphological investigations*

Scanning electron microscopy (SEM, Hitachi S-3000 N) was used to investigate the morphology of the cryo-fractured surface of the composites before and after ageing in DW. Back scattered electron mode with accelerating voltages of 20 kV was used.

2.6 Composite initial mechanical properties and as a function of time in PBS

Flexural (three-point bend) mechanical test was used to measure the mechanical properties of the composites. The effect of PG formulation on composite mechanical properties was investigated through changes in flexural strength, Young's modulus, and strain at maximum stress. Tests were performed on initially produced and PBS (Sigma Aldrich) conditioned specimens stored at 37°C and tested at days 7, 14, and 28. Mechanical testing was carried out on specimens in the dry state and the extent of their weight loss after PBS ageing was measured prior to mechanical testing, by first drying the specimens. Three repeat specimens were tested with a cross-head speed of 1 mm/min using a 1 kN load cell in accordance to ASTM D 790-95a:1996 (aspect ratio = 16) in an Instron mechanical testing instrument 5582 (Instron Ltd).

2.7 Cytocompatibility study: cell culture, seeding, and detection of cell viability

Murine MC3T3-E1 preosteoblasts (subclone 14) from American Type Culture Collection (CRL-2594 ATCC) were purchased from Cedarlane Labs and maintained in alpha modified Minimum Essential Medium (α-MEM, HyClone Laboratories Inc.) supplemented with 2 mM L-Glutamine (Invitrogen), 10% Newborn Calf Serum (NBCS, HyClone Laboratories Inc.) and 1% penicillin/ streptomycin (Invitrogen) at 37°C in humidified atmosphere of 5% CO_2. Both PG glass discs and PLA-PGF composites were assessed. Prior to cell seeding, PG glass discs (1 cm in diameter), PLA, PLA-Fe10 and PLA-Fe5Si5 and glass slide fragments (positive control), each with a surface area of 1 cm^2, were sterilised by immersion in absolute EtOH for 2 h. Specimens were then transferred to cell growth medium and conditioned overnight in a tissue culture incubator. MC3T3-E1 preosteoblasts were detached from tissue culture flasks (0.05% trypsin/0.02% EDTA), collected by centrifugal rotation (80 × *g*, 5 min) and seeded onto the samples at a density of 1.0×10^4 cells/cm^2. After 1, 4 and 7 days in culture, cells were detected by confocal laser scanning microscopy (CLSM, LSM 5, Carl Zeiss). To assess cell viability, cells were labelled using 1 mM calcein AM and 0.1 mM ethidium bromide homodimer-1 (LIVE/DEAD®, Invitrogen) in α-MEM for 30 min. Opaque materials were gently inverted (i.e. cell growth surface facing the microscope objective) onto a 50 mm Pelco glass bottom Petri dish (Ted Pella Inc.) and fluorescent-labelled cells were imaged using laser excitation (488 and 543 nm laser lines) and a baseline confocal z-stack was acquired at 1 Airy unit using a 20X EC Plan-Neofluar objective (0.5 N.A.). Maximum intensity projections were generated and analysed using NIH ImageJ v1.43 software.

2.8 Statistical analysis

A Student's *t* test was used to determine significant differences between two means using statistical significant level of $P < 0.05$.

3 Results

3.1 Glass characterisation

3.1.1 *Determination of crystalline phases in PG using X-ray diffraction*

Table 3 presents the identified phases from the crystalline state of the PGs. Calcium phosphate (α-(CaP_2O_6), ICCD No. 11-0039 and α-$Ca(PO_3)_2$, ICCD No. 17-0500) was

Table 3 Identification of phases in the crystallized Si and Fe doped PG formulations using X-ray diffraction

Glass code	Phase 1	Phase 2	Phase 3
Si10	α-(CaP_2O_6)	α-$Ca(PO_3)_2$	
Fe5Si5	α-$Ca(PO_3)_2$	α-(CaP_2O_6)	α-$CaSiO_3$
Fe10	α-(CaP_2O_6)	α-$Ca(PO_3)_2$	$CaFe_2O_4$

identified as the main phase of all the three PG formulations. Wollastonite ($CaSiO_3$, ICCD No. 3-0626) was also identified in Fe5Si5. In the case of Fe10, calcium iron oxide ($CaFe_2O_4$, ICCD No. 3-0040) was identified in addition to the calcium phosphate phases.

3.1.2 Surface properties of PGs

Table 4 summarises the mean contact angles for water and DII, polar, non-polar, and total surface energy, as well as the surface polarity of the PGs. Si10 glass showed the lowest water contact angle which increased with Fe_2O_3 content. In contrast, the DII contact angle was not significantly affected by the different compositions. While the polar surface energy and hence the surface polarity decreased by substituting SiO_2 with Fe_2O_3, the dispersive surface energies remained statistically unchanged. Consequently, the total surface energy increased with increasing amounts of SiO_2.

3.2 Structural characterization of as prepared PLA-PGF composites

ATR-FTIR spectra of PLA and PLA-PGF composites are presented in Fig. 1a. The band originating from stretching vibrations of C = O is situated at 1745 cm^{-1} for PLA, which decreased in PLA-Fe5Si5 compared to PLA and PLA-Fe10 (Fig. 1b). Differences between the spectra of PLA-Fe10 and PLA-Fe5Si5 can also be seen in the 1050–1250 cm^{-1} range attributed to C–O and C–O-C stretching vibrations. The absorbance ratio of the peak at 1745 cm^{-1}:1600 cm^{-1} decreased by 50% in PLA-Fe5Si5 compared to PLA and PLA-Fe10 (Fig. 1c).

The effect of PGF incorporation on the molecular weight of PLA was investigated using GPC. While the M_w of neat PLA was considerably reduced after processing, which could be associated with thermal degradation at the processing temperature (210°C, 30 min, and 38 bar), a 4-fold reduction in PLA M_w was observed in PLA-Fe5Si5 compared to as received PLA, which was also much greater than that in PLA-Fe10 (Fig. 1d). However, the polydispersity index of all the tested materials was not significantly changed.

3.3 Ageing of PLA-PGF composites in DW

Figure 2 shows the ion release, % of original mass, and pH change as a function of time in DW. At day 4 in DW, PO_4^{3-} and Ca^{2+} release was approximately 10-fold higher in PLA-Fe5Si5 compared to PLA-Fe10 (Fig. 2a, b, respectively). Fe^{3+} release (Fig. 2c) showed a similar trend but at a lower extent and greater amount was released from PLA-Fe5Si5 compared to PLA-Fe10. Si^{4+} release occurred within 8 h, which was more rapid compared to the other ionic species which indicated a 48–72 h delay prior to release (Fig. 2d).

While neat PLA demonstrated no weight change across the entire conditioning period in DW, PLA-Fe10 demonstrated a minor degree of weight gain (<10%) by day 56 (Fig. 2e). In contrast, after 48 h, there was a significant weight gain in PLA-Fe5Si5 which increased by up to 50% by day 56. The delay in weight gain coincided with the delay in ionic release (Fig. 2a–c). Based on the final dry weight of the composites at day 56 (Table 5), there was a 2.23 and 23.41% weight loss for PLA-Fe10 and PLA-Fe5Si5, respectively. Residual glass was estimated at 93.36 and 26.17 wt.% for PLA-Fe10 and PLA-Fe5Si5, respectively.

The pH of DW remained relatively unchanged in the presence of PLA and PLA-Fe10 (Fig. 2f). In the case of PLA-Fe5Si5, there was a decrease in pH, which initiated after 48 h. The pH became increasingly acidic (~pH 3.5)

Table 4 Contact angle measurements with ultrapure water (CA^{H2O}) and diiodomethane (CA^{DII}), Total surface energy (SE^t) with the dispersive (SE^d) and polar (SE^p) parts of different phosphate glass compositions according to the OWRK method, and surface polarity ($X^p = SE^p/SE^t$). Si10 glass showed the lowest CA^{H2O} which increased significantly by substituting SiO_2 with Fe_2O_3 in the glass formulation; whereas, the contact angle for DII was unchanged. On the other hand, SE^t decreased significantly by substituting SiO_2 with Fe_2O_3. In addition, the substitution of SiO_2 with Fe_2O_3 resulted in reduced surface polarity

Sample	CA^{H2O}	CA^{DII}	SE^t	SE^d	SE^p	X^p
Si10	10.37 ± 5.99	38.42 ± 3.19	71.97 ± 1.02	28.88 ± 1.66	43.1 ± 2.54	0.60 ± 0.02
Fe5Si5	*22.85 ± 1.2	37.77 ± 2.04	*68.43 ± 0.55	29.78 ± 0.81	*38.71 ± 0.86	*0.56 ± 0.01
Fe10	**42.85 ± 1.72	37.2 ± 1.7	**58.54 ± 0.73	31.91 ± 0.98	**26.62 ± 1.53	**0.45 ± 0.02

* Statistically significant compared to Si10 ($P < 0.05$)

** Statistically significant compared to Fe5Si5 ($P < 0.05$)

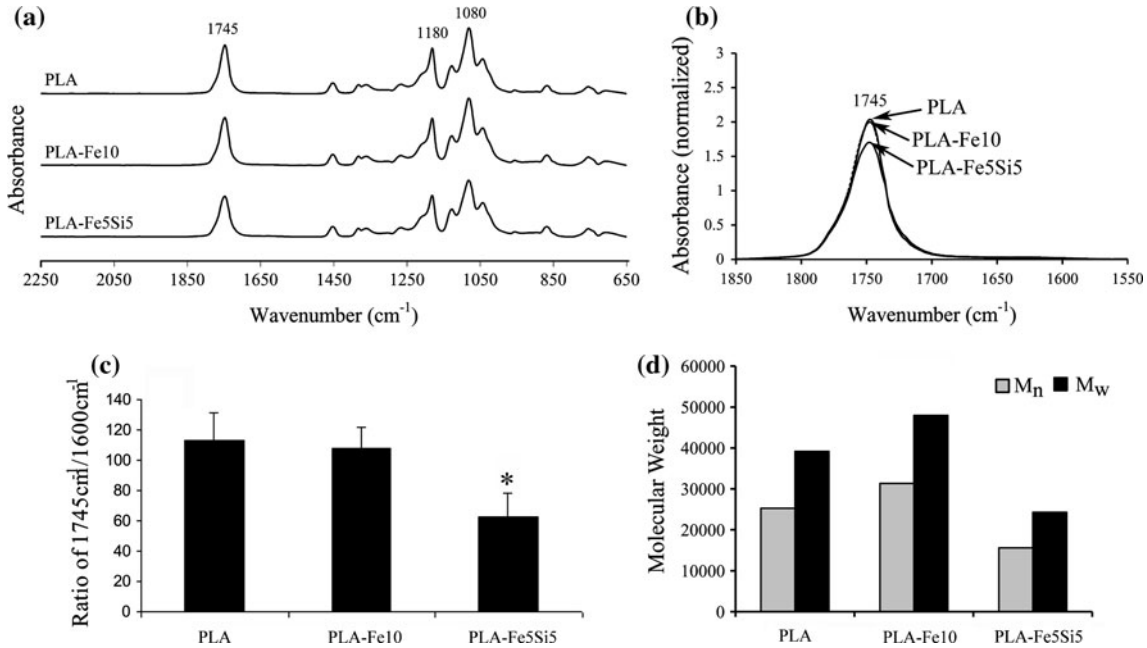

Fig. 1 ATR-FTIR analysis: **a** ATR-FTIR spectra of as processed PLA and PLA-PGF composites. PLA-Fe5Si5 showed a decrease in the absorbance of the peaks at 1745 (C = O stretching), 1080 and 1180 cm^{-1} (C–O/C–C stretching). **b** The superimposition of the peak at 1745 cm^{-1} indicating the reduction in its intensity in the case of PLA-Fe5Si5 when compared to PLA and PLA-Fe10. **c** The absorbance ratio of 1745/1600 cm^{-1}; there was a statistically significant reduction in this ratio in the case of PLA-Fe5Si5 ($P < 0.05$). **d** Gel permeation chromatography: Number (M_n) and weight (M_w) average molecular weight of PLA and PLA in PLA-PGF composites. There was a greater reduction of the molecular weight of as processed PLA-Fe5Si5 relative to PLA and PLA-Fe10

up to 336 h after which, it started to recover (back towards neutral) due to medium replacement at each time interval and reductions in phosphate release (Fig. 2a).

3.4 Morphological characterisation

SEM micrographs of the morphology of as-processed PLA-PGF composites demonstrated the random distribution of PGFs within the PLA matrix (Fig. 3a, b). After 56 days immersion in DW, both channels and residual glass fibres were observed in PLA-Fe10 (Fig. 3c, d). As a consequence of the increased solubility of Fe5Si5 PGF, PLA-Fe5Si5 demonstrated fewer remaining fibres. In addition there was a substantial presence of matrix associated voids (Figs. 3e, f).

3.5 Mechanical property changes in PBS

Figure 4a shows the weight change in the composites as a function of immersion time in PBS. At Day 28, there was a loss of 11.69 wt.% in the final dry weight of PLA-Fe5Si5, compared to 0.84 wt.% for PLA-Fe10. Mechanical characterisation of as processed composites demonstrated 2.5- and 2.2-fold increases in the initial flexural strength and modulus through reinforcement with PGF (Fig. 4b, c). The strain at maximum stress (Fig. 4d) did not show a statistically significant difference.

At days 7 and 28 in PBS, the flexural strength of the PLA-PGF composites decreased significantly ($P < 0.05$). The reduction was greater in PLA-Fe5Si5 (75 and 94% at days 7 and 28, respectively) compared to PLA-Fe10 (49 and 62% at days 7 and 28, respectively). There was a similar trend in the reduction of the Young's modulus of the composites. Strain at maximum stress of PLA-Fe10 remained relatively unchanged with immersion time whereas that of PLA-Fe5Si5 decreased significantly at day 7. There was no statistically significant difference in the strain at maximum stress between day 7 and 28 for both PLA-Fe10 and PLA-Fe5Si5.

3.6 Cytocompatibility assessment of PG and PLA-PGF composites

To assess the cytocompatibility of PG and PLA-PGF composites, the viability of MC3T3-E1 preosteoblasts grown on PG glass discs, PLA-Fe10 and PLA-Fe5Si5 was compared to cells grown on either neat PLA or microscope glass slides. After days 1, 4 or 7, cells were stained using calcein-AM (green fluorescent cells) and ethidium bromide homodimer-1 (red fluorescent cell nuclei) and Live/Dead fluorescence staining was detected by CLSM. Maximum intensity projections of z-stacks obtained by CLSM revealed viable, calcein-AM labelled MC3T3-E1 cells attached to the surfaces of the PG discs (Fig. 5) as well as

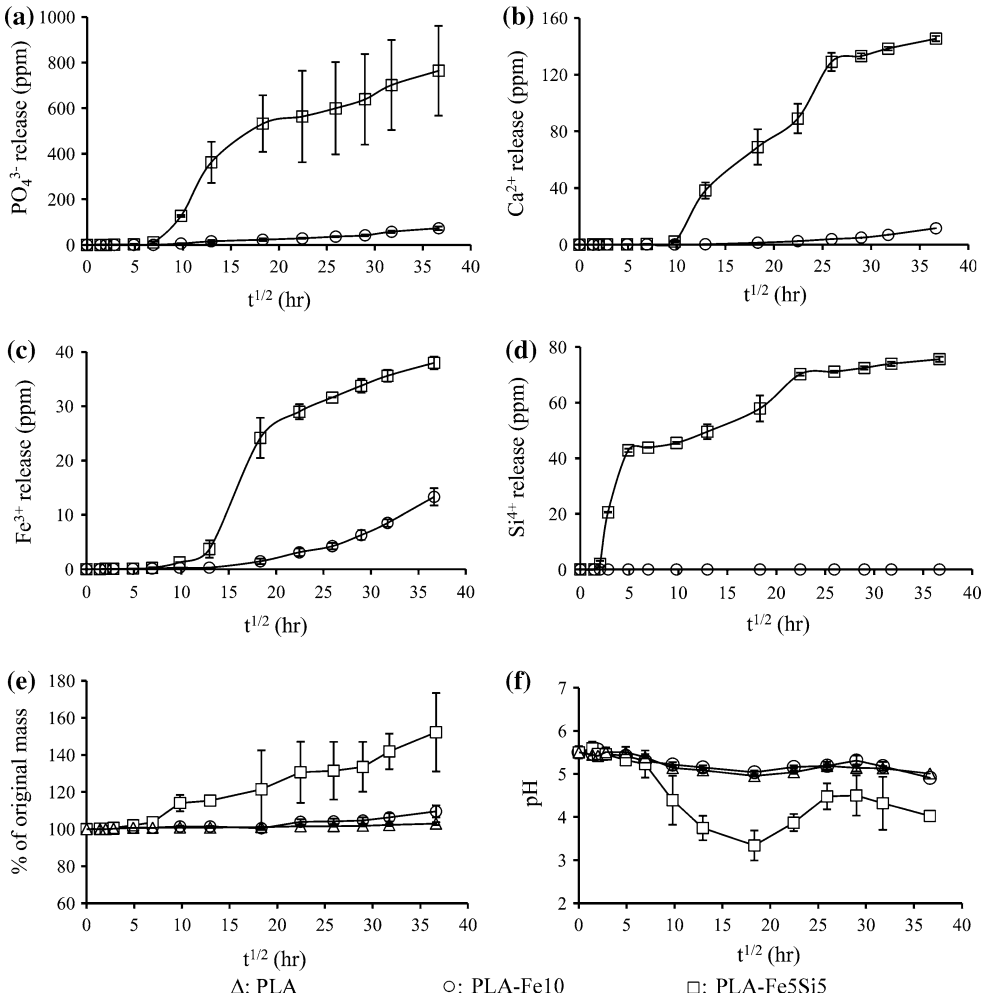

Fig. 2 Ageing of PLA and PLA-PGF composites in DW incubated for up to 56 days at 37°C. **a** PO_4^{3-}, **b** Ca^{2+}, **c** Fe^{3+}, and **d** Si^{4+} ion release. Anion and cation release was higher in PLA-Fe5Si5 compared to PLA-Fe10. **e** Weight loss, and **f** pH change of the immersion environment. PLA-Fe5Si5 composites underwent a significantly higher increase in weight relative to PLA-Fe10 and PLA. There was a relatively greater reduction in the pH of DW in the case of PLA-Fe5Si5

Table 5 Weight loss and residual glass fibres of the samples in the final dry weight of the specimens after 56 days incubation in DW at 37°C. At day 56, there were ~7 and 74 wt. % reduction of Fe10 and Fe5Si5, respectively

Material	% of original mass	Remaining glass (wt.%)
PLA	99.91 ± 0.07	–
PLA-Fe10	97.77 ± 0.73	93.36
PLA-Fe5Si5	76.59 ± 4.23	26.17

PLA, PLA-PGF composites (Fig. 6) and microscope glass slides at days 1, 4 and 7 in culture. At day 1, live MC3T3-E1 preosteoblasts attached to the surface of each of the samples. Fe10 and Fe5Si5 showed a slightly greater extent of MC3T3-E1 preosteoblast attachment compared to the control (Fig. 5). The number of necrotic/apoptotic dead cells, indicated by EtBr-1 nucleic binding, was very low and comparable for each condition. At day 4, as the centre of the PG glass discs was covered by cells (data not shown), confocal images were captured on the edge to reveal the growing cells (Fig. 5). Cells were viable on the surfaces of Fe10 and Fe5Si5, with a limited number of dead cells observed on the PG glass discs compared to the control. However, at day 7 the cells completely covered the surfaces of both compositions. PLA and the PLA-PGF composites showed a similar extent of MC3T3-E1 preosteoblast attachment whereas cell adhesion and spreading onto the microscope glass slide was greater (Fig. 6). Unlike PLA and microscope glass slide, cell alignment was detected along the PGF within PLA-PGF composites. After 4 days of cell growth, the number of live cells increased and approached confluence, whilst only a few necroctic/apoptotic cells were detected. At day 7, the surface of all the tested specimens was covered by living cells, and the cell alignment effect of the PGF was still evident within the PLA-PGF composites compared to neat PLA and microscope glass slide.

4 Discussion

Biodegradable composites of tailored properties for applications in bone augmentation and regeneration could be

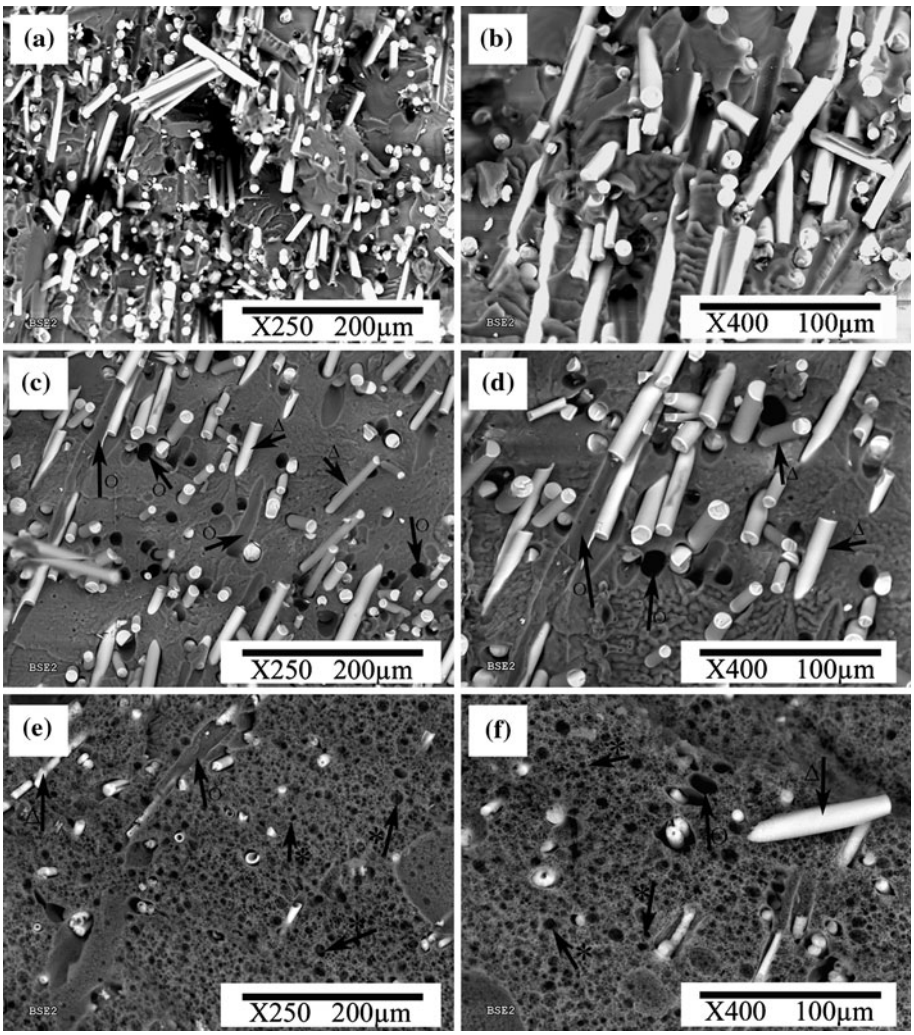

Fig. 3 Morphological characterisation: SEM micrographs of cryo-fractured specimens as processed and after conditioning in DW at different magnifications: (**a**, **b**) as processed PLA-PGF composites, (**c** and **d**) PLA-Fe10 and (**e** and **f**) PLA-Fe5Si5 at day 56 in DW. As processed composites showed randomly dispersed and attached glass fibres in the polymeric matrix. After 56 days of immersion in DW, a majority of the PGF remained in the microstructure of PLA-Fe10 due to very low degradation rate of Fe10 glass fibres, and channel formation can also be seen as a result of dissolved fibres. In contrast, most of the glass fibres were dissolved in PCL-Fe5Si5 due to considerably higher degradation rate of Fe5Si5 glass fibres. Void formation was observed in the PLA matrix in PLA-Fe5Si5. (*Arrows* with *triangle*: PGF, *Arrows* with *circle*: Channels, *Arrows* with *asterisk*: Voids)

produced using soluble PGFs and biodegradable polymers, such as PLA. PG composition dictates its degradation characteristic. For example, it has been demonstrated that the presence of Fe_2O_3 strengthens the cross-linking between the glass polyphosphate chains producing hydration resistant bonds, which results in higher glass stability [14, 23]. In contrast, Si breaks down the PG network, lowering the stability and increasing the degradation rates [14]. In addition, the polar interactions at the glass surface are influenced by the composition. It has been shown that Fe_2O_3 incorporation resulted in reduced surface polarity, and hence surface energy [18]. Since SiO_2 disrupts the network, and can form hydroxyl groups (Si–OH) at the surface of PG, the aim of this study was to investigate the effect of Fe_2O_3 and SiO_2 incorporation on the surface properties of PG. Glass surface properties also impacts the nature of interfacial interaction of fibre and matrix, which affects composite properties. Therefore, this study also investigated the influence of incorporating Fe and Si doped PGFs on PLA-PGF composite properties.

X-ray diffraction revealed the presence of calcium phosphate (α-(CaP_2O_6) and α-$Ca(PO_3)_2$) as the main phase of the crystallised PGs. $CaSiO_3$ and $CaFe_2O_4$ were also identified in Fe5Si5 and Fe10 PGs, respectively. Although these phases are present in the crystalline state of the PG, the formation of different phases could be an indication of structural difference which affects the bulk properties.

By altering the composition, the hydrophilicity as well as surface energy of the glasses can be controlled, which significantly affect the hydrolysis driven solubility of PGs, as well as their interactions with the polymer matrix. This study has shown that lower contact angles were obtained on the surface of Si10 and Fe5Si5 compositions when using water as the test liquid due to the polar characteristic of PGs, which can be attributed to the P–O-P bonds [24]. However, substitution of SiO_2 with Fe_2O_3 in the glass formulation significantly increased the contact angle of water, while it decreased the total surface energy, as well as the polar characteristic of the PG. This may be attributable to the reduction in the concentration of hydroxyl groups at

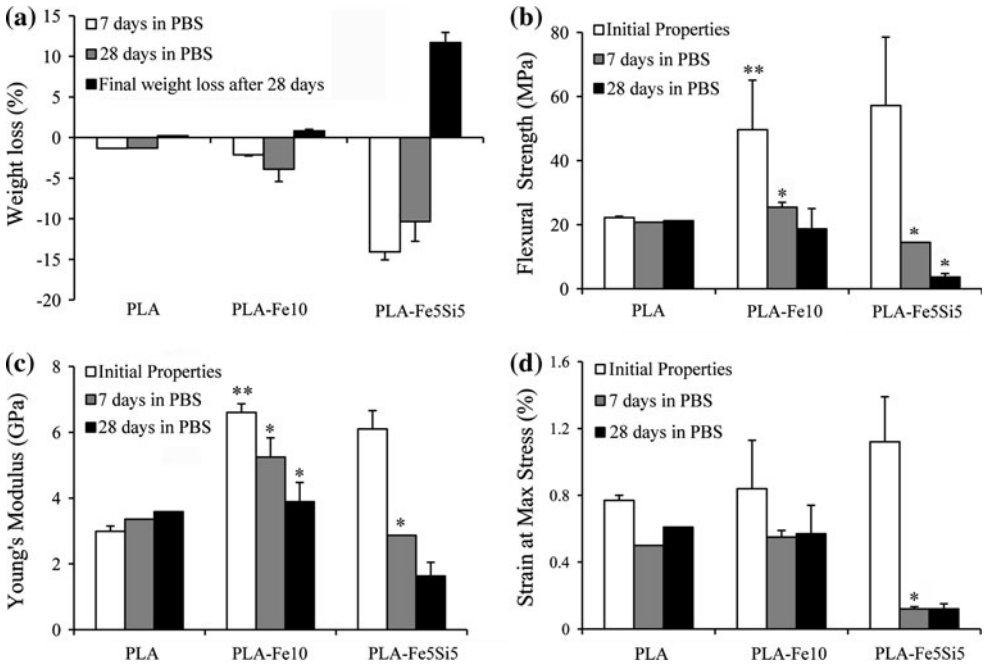

Fig. 4 Mechanical properties and weight loss over the course of 28 days in PBS: **a** Weight loss of PLA and PLA-PGF composites at days 7 and 28, and final dry weight at day 28. **b** flexural strength **c** flexural modulus, and **d** strain at maximum stress of PLA and PLA-PGF composites as produced and post PBS conditioning. Initial flexural strength increased significantly ($P < 0.05$) via the addition of PGF. While flexural modulus increased significantly ($P < 0.05$), there was no significant change in strain at maximum stress. After ageing in PBS, the decrease in mechanical properties was considerably higher for Fe5Si5 containing composites compared to Fe10 containing composites. * Statistically significant difference for same time point compared with previous sample ($P < 0.05$). ** Statistically significant difference for same sample compared to previous time point ($P < 0.05$

the surface of the PG with a decrease in SiO_2. The surface energies of Si10 and Fe5Si5 was 72 and 68.4 mN/m, respectively, which are greater than what has been reported for Bioglass® (54.7 mN/m [25]) and within the range reported for iron containing PGs in the P_2O_5-CaO-Na_2O-Fe_2O_3 systems with 0–5 mol.% Fe_2O_3 (61.2–76 mN/m) [18]. However, the surface polarity of Si10 and Fe5Si5 compositions were 0.60 and 0.56, respectively, which were higher than that of these PGs (0.43–0.51) [18] indicating the effect of SiO_2 on increasing surface polarity. The greater hydrophilicity of Si10 and Fe5Si5 PGs increases their wettability and water adsorption leading to an increase in the concentration of Si–OH groups at the surface.

Hydroxyl group formation at the surface of PGs through SiO_2 incorporation increased the potential for interfacial interaction between the fibres and PLA matrix. As an indication of PLA degradation in the as prepared composites, FTIR spectra of PLA-Fe5Si5 revealed a reduction in the absorbance of the carbonyl peak at 1745 cm^{-1} compared to PLA; whereas, it did not change for PLA-Fe10. Reductions were also observed in the peaks around 1080 and 1180 cm^{-1} which are attributed to C–O/C–C stretching peaks. A previous study [19] also demonstrated similar behaviour with Si doped PG particulates in PCL, where a potential reaction took place between Si10 and the ester bond in the polyester at elevated temperature causing chain-scission and forming carboxylate by-products, which decreased the matrix molecular weight. The high surface energy of Si10 composition, as measured in this study, combined with particulate surface area enhanced the reaction with the PCL ester bond [19]. While carboxylate by-products were not indicated in this study, possibly due to the presence of SiO_2 in the quaternary system (Fe5Si5) with lower surface energy and polarity compared to Si10, combined with the relatively lower surface area of the fibres than particulates, the reduction in the ratio of 1745 cm^{-1}:1600 cm^{-1} indicated PLA chain scission. The reduction in PLA M_w, particularly in the case of PLA-Fe5Si5 confirmed matrix degradation, which was greater than that in neat PLA and PLA-Fe10. Blaker et al. [20] confirmed the induction of polyester degradation through silicate-based bioactive glasses incorporated at elevated temperatures. A reduction in the M_w of the matrix by incorporation of bioactive glass particles into poly(ε-caprolactone-co-DL-lactide) has also been reported [26].

The influence of glass surface properties and PLA matrix degradation on the ageing behaviour of the composites was demonstrated through ion release and weight

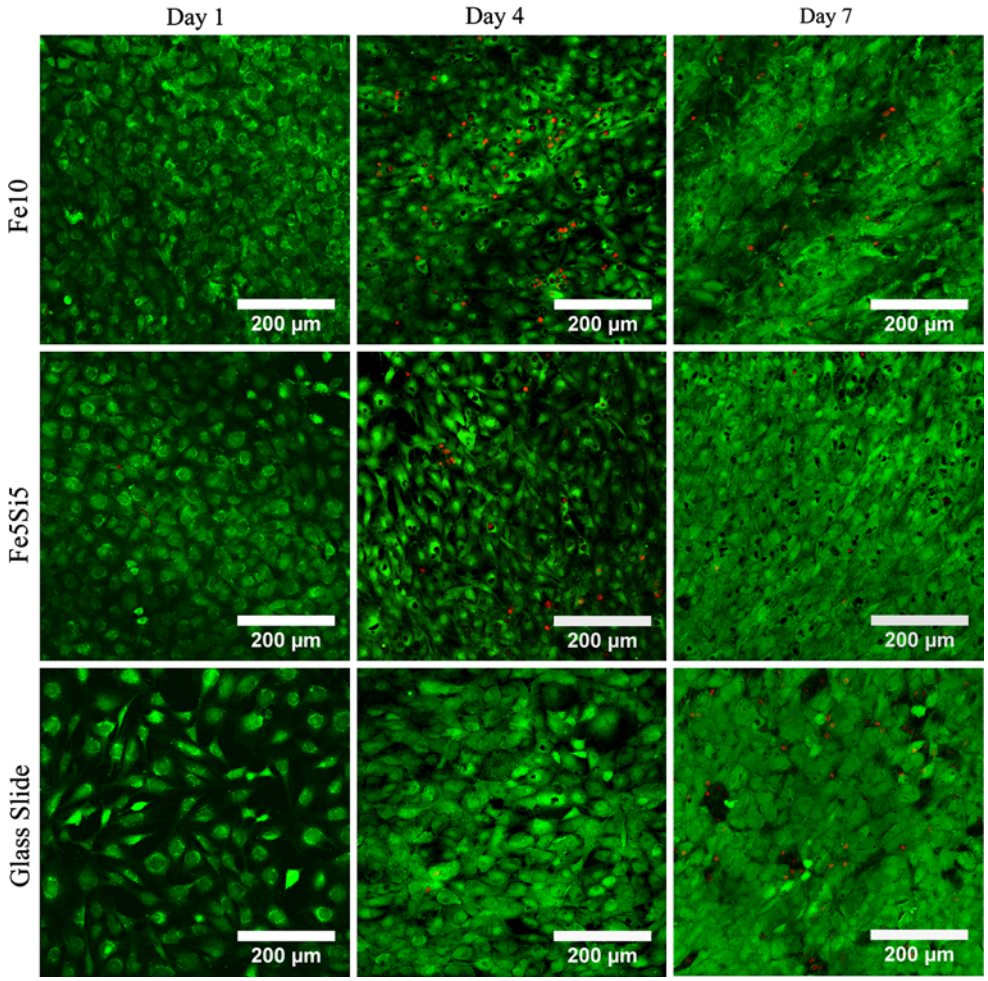

Fig. 5 Live/Dead staining of MC3T3-E1 preosteoblasts seeded on PG discs: Cells were stained using calcein-AM (*green*) and ethidium bromide homodimer-1 (*red*) at days 1, 4 and 7, and fluorescence was detected by CLSM. Fe10 and Fe5Si5 PG discs showed a similar extent of MC3T3-E1 preosteoblast attachment higher than the microscope glass on day 1. Since the center of the specimen was covered by cells, day 4 images were captured on the edge of the samples showing the growing cells. The growing cells completely covered the surface of the specimens at day 7

loss in deionised water. PLA-Fe5Si5 was found to have a significantly greater anion and cation release compared to PLA-Fe10 as reflected by their ion release rates (Supplementary Table 1). As previously reported, the release rates of PO_4^{3-} and Ca^{2+} ions were in line with the rate of glass dissolution [27]. While Si^{4+} release was due to the presence of Fe5Si5 fibres, Fe^{3+} also showed a similar dependency on the presence of Si in the formulation. The latter can be explained by the rate of ion release dependence on water uptake. The addition of Si increased the glass solubility and water ingress due to channel formation. The greater exposure of glass fibres to water resulted in greater dissolution and an increase in Fe^{3+} ion release. Since neat PLA did not gain weight, it can be assumed that the water uptake occurred at the fibre-matrix interface and within the degraded matrix, particularly in the case of PLA in PLA-Fe5Si5. Water uptake was higher in PLA-Fe5Si5 compared to PLA-Fe10 due to higher hydrophilicity and surface energy of Fe5Si5. In addition, in the case of PLA-Fe5Si5, matrix degradation may have resulted in the formation of voids upon ageing in DW leading to more water ingress. The voids may be due to the leaching of low molecular weight species produced through PLA matrix degradation. SEM images of PLA-Fe5Si5 after immersion in water displayed void formation within the PLA matrix, which were not observed in either neat PLA (data not shown) or in PLA-Fe10. SEM micrographs confirmed that after 56 days ageing, a much greater amount of the Fe5Si5 fibres dissolved compared to Fe10 fibres. The extensive dissolution of Fe5Si5 fibres led to the creation of channels in the microstructure of the composites, which may also provide interconnectivity within the structure, and allow the

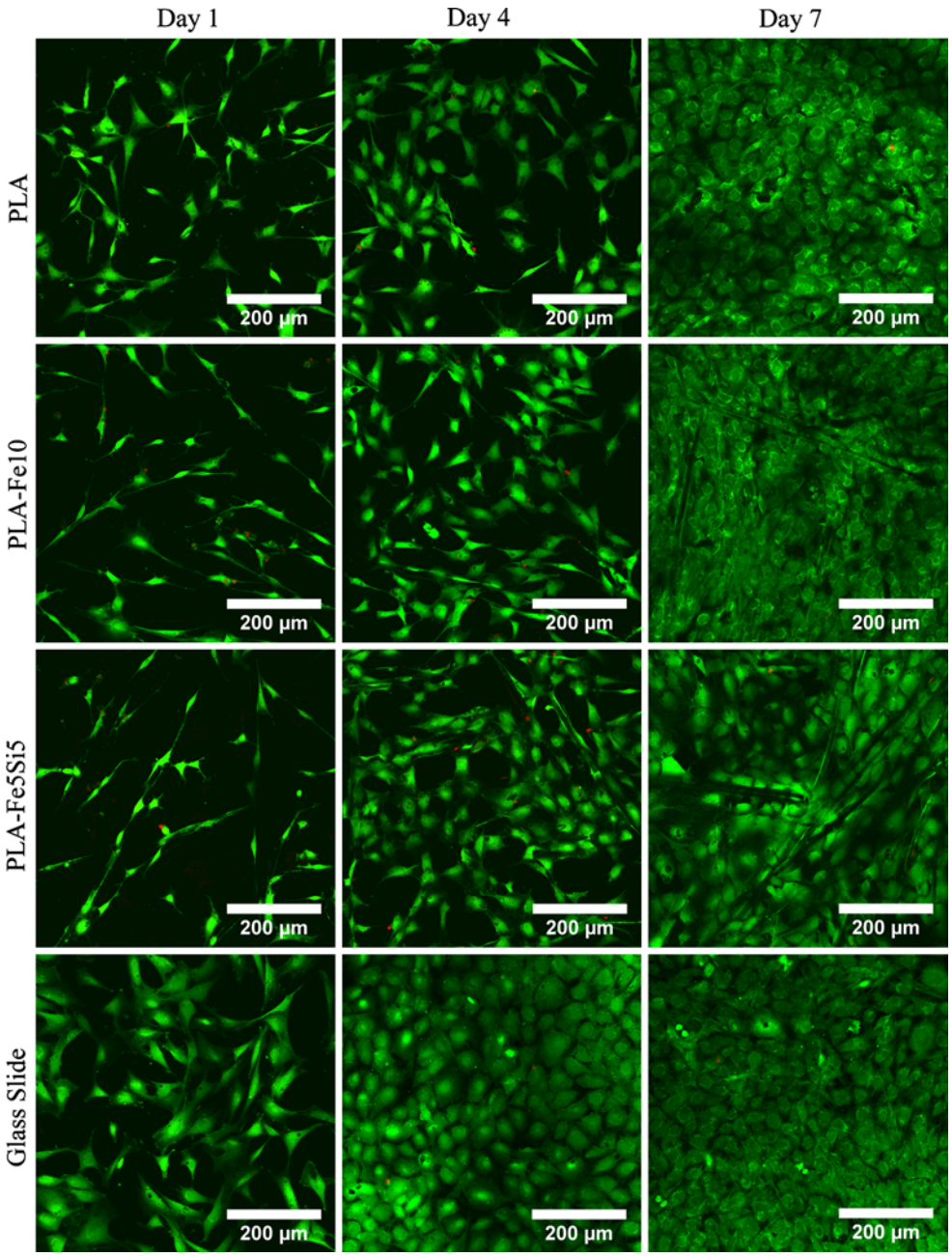

Fig. 6 Live/Dead staining of MC3T3-E1 preosteoblasts seeded on PLA-PGF composites: Cells were stained using calcein-AM (*green*) and ethidium bromide homodimer-1 (*red*) at days 1, 4 and 7, and fluorescence was detected by CLSM. PLA and the PLA-PGF composites showed a similar extent of MC3T3-E1 preosteoblast attachment on day 1, while cell adhesion and spreading onto microscope glass was greater. However, cell alignment along the PGF was observed on PLA-PGF composites indicating tendency of the cells towards the PGF. The number of live cells increased and approached confluence similarly on the surface of all tested specimens after 4 and 7 days in culture

release of ionic species from residual glass fibres. Higher degradation rate in Fe5Si5 containing composites led to a more rapid rate of pH reduction compared to PLA-Fe10. The higher release rate of the phosphate species led to an acidic medium through the formation of phosphoric acid [18].

Flexural mechanical analysis showed that incorporating PGF into PLA led to a considerable increase in the flexural strength and Young's modulus, resulting in values within the ranges found for trabecular bone [28–30] (approximately 40 MPa and 2 GPa for strength and modulus, respectively). These increases were attributed to the higher levels of stress transfer expected from fibre reinforcement, in comparison to particulate reinforcement. Both the length-to-diameter ratio as well as the larger shear surface

of individual reinforcements, led to a higher modulus and reduced ductility. In contrast, Si and Fe doped PG particulates did not increase the strength when incorporated into PCL [19]. It has also been shown that incorporation of various SiO_2 bioactive glass particulates into poly(α-hydroxyesters) at elevated temperatures resulted in a reduction in the strength and modulus and increased degradation of the composite matrices [20, 26, 31].

As a consequence of ageing in PBS, the reduction in mechanical properties was greater for PLA-Fe5Si5 compared to PLA-Fe10, which can be attributed to greater weight loss and channel generation, as well as PLA matrix degradation in PLA-Fe5Si5. The lower solubility rate of Fe10 was reflected by the greater retention of the mechanical properties of PLA-Fe10 (~22 MPa and 4.2 GPa for strength and modulus, respectively, at day 28), which were still within the range for trabecular bone.

The cytocompatibility of PGs has been demonstrated to be dependent on their solubility rate [32–34]. For example, Skelton et al. [35] showed that as a consequence of their rapid dissolution, PGs of the system $50P_2O_5$-(50-x) CaO-xNa_2O, $x = 2$–10 mol.% adversely affected the viability of osteoblasts. PGs with lower degradation rates demonstrated better cytocompatibility, viability, and proliferation, and early differentiation was only observed at higher CaO content (48 mol.%). However, the incorporation of metal oxides, such as TiO_2 and Fe_2O_3, has been shown to improve biocompatibility by controlling the glass degradation and ionic release rates hence maintaining the appropriate pH favoured by the osteoblasts [32, 36]. Bitar et al. [32] investigated the biological response of PGs in the $50P_2O_5$-46CaO-xNa_2O-yFe_2O_3 ($y = 0$–3 mol.%) system using primary human osteoblasts and fibroblasts. Replacing Na_2O with Fe_2O_3 resulted in significant improvement in cell viability, proliferation and differentiation. In addition, the positive effect of Si on bone metabolism has been demonstrated, and its substitution into calcium phosphate ceramics, e.g. hydroxyapatite (HA) or tricalcium phosphate, has demonstrated enhanced biological responses [37]. However, the direct influence of Si on osteoblastic cells is still under question due to the lack of evidence of therapeutic release of Si from these calcium phosphates [38]. The incorporation of Si into soluble PGs can also control the release of phosphorous and calcium ions which may affect the biological behaviour of osteoblasts. For example, the release of phosphorous and calcium ions from HA coatings has been shown to influence osteoblast responses, where enhanced osteoblast differentiation was observed with additional calcium concentration; while additional phosphorous was suggested to slow down the differentiation and mineralisation [39]. In this study, MC3T3-E1 cells remained viable and approached confluency on Fe10 and Fe5Si5 PG discs compared to cells grown on microscope glass slides. The addition of Si and Fe containing PGF into PLA altered the preosteoblastic cytocompatibility of the materials and cell alignment along the PGF was observed indicating the tendency of preosteoblasts towards PGF. This could be due to the release of favourable ions from the PGF which needs further investigations. Similar study using MG63 cell line on PLA-PGF ($50P_2O_5$-40CaO-5Na_2O-5Fe_2O_3) composite have shown cell attachment and viability yet to a lower extent compared to this study [40].

5 Conclusions

PG composition can greatly influence its bulk and surface properties, which would also affect composite properties when incorporated as fillers. In this study, the effect of SiO_2 and Fe_2O_3 doping on PG surface properties, and its influence on the composite properties when incorporated into PLA as PGF were investigated. The addition of SiO_2 in the PG formulation resulted in higher hydrophilicity, surface energy, and surface polarity. Increased surface energy and polarity increased the interaction between the Fe5Si5 and the polymer matrix reducing the molecular weight of the PLA matrix by chain-scission, which did not occur in PLA-Fe10 (SiO_2 free PGF). Increased hydrophilicity resulted in more rapid hydrolysis of the glass resulting in higher degradation and ion release in the composite system, as well as increased water uptake. Initially, PGF incorporation increased the strength and modulus of the composites by 2.5- and 2.2-fold, respectively, compared to neat PLA. The reduction in mechanical properties after ageing in PBS was higher for PLA-Fe5Si5 compared to PLA-Fe10 due to higher degradation rate of Fe5Si5 fibres. In addition, MC3T3-E1 preosteoblasts showed that the investigated composites were cytocompatible and cells preferably aligned along the phosphate glass fibres in PLA-PGF composites.

Acknowledgements This work was funded by the Canadian Natural Sciences and Engineering Research Council, Le Fonds québécois de la recherche sur la nature et les technologies, McGill University Faculty of Engineering Hatch Faculty Fellowship, and Canada Foundation for Innovation: Leaders Opportunity Fund. Funding for Maziar Shah Mohammadi was also partly supported by a McGill Engineering Doctoral Award. The authors thank Saurav Mohapatra and Hye-Lim Choi for their assistance in this work. Martin N. Bureau is a member of the Groupe de Recherche en Sciences et Technologies Biomédicales (Fonds de recherche en santé du Québec).

References

1. Maquet V, Boccaccini AR, Pravata L, Notingher I, Jerome R. Preparation, characterization, and in vitro degradation of

bioresorbable and bioactive composites based on Bioglass®-filled polylactide foams. J Biomed Mater Res part A. 2003;66A: 335–46.
2. Onal L, Cozien-Cazuc S, Jones IA, Rudd CD. Water absorption properties of phosphate glass fibre-reinforced poly-ε-caprolactone composites for craniofacial bone repair. J Applied Polymer Sci. 2008;107:3750–5.
3. Verrier S, Blaker JJ, Maquet V, Hench LL, Boccaccini AR. PDLLA/Bioglass^R composites for soft-tissue and hard-tissue engineering: an in vitro cell biology assessment. Biomaterials. 2004;25:3013–21.
4. Georgiou G, Mathieu L, Pioletti DP, Bourban PE, Månson JAE, Knowles JC, Nazhat SN. Polylactid acid-phosphate glass composite foams as scaffolds for bone tissue engineering. J Biomed Mater Res B. 2006;322-31.
5. Lin ASP, Barrows TH, Cartmel SH, Guldberg RE. Microarchitectural and mechanical characterization of oriented porous polymer scaffolds. Biomaterials. 2003;24:481–9.
6. Boccaccini AR, Blaker JJ, Maquet V, Day RM, Jerome R. Preparation and characterization of poly(lactic-co-glycolide) (PLGA) and PLGA/Bioglass composites tubular foam scaffolds for tissue engineering applications. Mater Sci Eng C. 2005;25: 23–31.
7. Blaker JJ, Maquet V, Jerome R, Boccaccini AR, Nazhat SN. Mechanical properties of highly porous PDLLA/Bioglass® composite foams as scaffolds for bone tissue engineering. Acta Biomater. 2005;1:643–52.
8. Engleberg I, Kohn J. Physico-mechanical properties of degradable polymers used in medical applications: a comparative study. Biomaterials. 1991;12:292–304.
9. Jiang G, Evans ME, Jones IA, Rudd CD, Scotchford CA, Walker GS. Preparation of poly(ε-caprolactone)/continuous bioglass fibre composite using monomer transfer moulding for bone implant. Biomaterials. 2005;26:2281–8.
10. Yaszemski MJ, Powers JM, Mikos AG. Hydroxyapatite fiber reinforced poly(alpha-hydroxy ester) foams for bone regeneration. Biomaterials. 1998;19:1935–43.
11. Dupraz AMP, de Wijn JR, vd Meer SAT, de Groot K. Characterization of silane-treated hydroxyapatite powders for use as filler in biodegradable composites. J Biomed Mater Res. 1996;30: 231–8.
12. Knowles JC. Phosphate based glasses for biomedical applications. J Mater Chem. 2003;13:2395–401.
13. Abou Neel EA, Pickup DM, Valappil SP, Newport RJ, Knowles JC. Bioactive functional materials: a perspective on phosphate-based glasses. J Mater Chem. 2009;19:690–701.
14. Patel A, Knowles JC. Investigation of Silica-iron-phosphate glasses for tissue engineering. J Mater Sci Mater Med. 2006; 17:937–44.
15. Gao H, Tan T, Wang D. Effect of composition on the release kinetics of phosphate controlled release glasses in aqueous medium. J controlled release. 2004;96:21–8.
16. Franks K, Abrahams I, Knowles JC. Development of soluble glasses for biomedical use part 1: in vitro solubility measurement. J Mater Sci Mater Med. 2000;11:609–14.
17. Ahmed I, Lewis M, Olsen I, Knowles JC. Phosphate glasses for tissue engineering: part 2. Processing and characterization of a ternary-based P_2O_5-CaO-Na_2O glass fibre system. Biomaterials. 2004;25:501–7.
18. Abou Neel EA, Ahmed I, Blaker JJ, Bismarck A, Boccaccini AR, Lewis MP, Nazhat SN, Knowles JC. Effect of iron on the surface, degradation and ion release properties of phosphate-based glass fibres. Acta Biomater. 2005;1:553–63.
19. Shah Mohammadi M, Ahmed I, Marelli B, Rudd C, Bureau MN, Nazhat SN. Modulation of polycaprolactone composite properties through incorporation of mixed phosphate glass formulations. Acta Biomater. 2010;6:3157–68.
20. Blaker JJ, Bismarck A, Boccaccini AR, Young AM, Nazhat SN. Premature degradation of poly(α-hydroxyesters) during thermal processing of Bioglass® containing composites. Acta Biomater. 2010;6:756–62.
21. Blaker JJ, Maquet V, Boccaccini AR, Jérôme R, Bismarck A. Wetting of bioactive glass surfaces by poly(α-hydroxyacid) melts: interaction between Bioglass® and biodegradable polymers. E-polymers. 2005;23:1–13.
22. ASTM Standard D2584–94, Test method for ignition loss of cured reinforced resins. West Conshohocken PA: ASTM international 1994; <www.astm.org>.
23. Ahmed I, Collins CA, Lewis M, Olsen I, Knowles JC. Processing, characterization and biocompatibility of iron-phosphate glass fibres for tissue engineering. Biomaterials. 2004;25:3223–32.
24. Abou Neel EA, Chrzanowski W, Knowles JC. Effect of increasing titanium dioxide content on bulk and surface properties of phosphate-based glasses. Acta Biomater. 2008;4:523–34.
25. Park JM, Kim DS, Kim SR. Interfacial properties and microfailure degradation mechanisms of bioabsorbable fibres/poly-L-lactide composites using micromechanical test and non-destructive acoustic emission. Comp Sci Tech. 2003;63:403–19.
26. Rich J, Jaakkola T, Tirri T, Närhi T, Yli-Urpo A, Seppälä J. In vitro evaluation of poly(ε-caprolactone-co-D, L-lactide)/bioactive glass composites. Biomaterials. 2002;23:2143–50.
27. Ahmed I, Lewis MP, Nazhat SN, Knowles JC. Quantification of anion and cation release from a range of ternary phosphate-based glasses with fixed 45 mol% P_2O_5. J Biomater Appl. 2005;20:65–80.
28. Mondrinos MJ, Dembzynski R, Lu L, Byrapogu VKC, Wootton DM, Lelkes PI, et al. Porogen-based solid freeform fabrication of polycaprolactone-calcium phosphate scaffolds for tissue engineering. Biomaterials. 2006;7:4399–408.
29. Teo JCM, Si-Hoe KM, Keh JEL, Teoh SH. Correlation of cancellous bone microarchitectural parameters from microCT to CT number and bone mechanical properties. Mater Sci Eng C. 2007;27:333–9.
30. Vitins V, Dobelis M, Middleton J, Limbert G, Knets I. Flexural and creep properties of human jaw compact bone for FEA studies. Comput Methods Biomech Biomed Engin. 2003;6:299–303.
31. Niemelä T, Niiranen H, Kellomäkii M, Törmälä P. Self-reinforced composites of bioabsorbable polymer and bioactive glass with different bioactive glass contents. Part I. Initial mechanical properties and bioactivity. Acta Biomater. 2005;1:235–42.
32. Bitar M, Knowles JC, Lewis MP, Salih V. Soluble phosphate glass fibres for repair of bone-ligament interface. J Mater Sci Mater Med. 2005;16:1131–6.
33. Bitar M, Salih V, Mudera V, Knowles JC, Lewis M. Soluble phosphate glasses: in vitro studies using human cells of hard and soft tissue origin. Biomaterials. 2004;25:2283–92.
34. Shah R, Sinanan ACM, Knowles JC, Hunt NP, Lewis MP. Craniofacial muscle engineering using a 3-dimensional glass fibre constructs. Biomaterials. 2005;26:1497–505.
35. Skelton KL, Glenn JV, Clarke SA, Georgiou G, Valappil SP, Knowles JC, Nazhat SN, Jordan GR. Effect of phosphate-based glass ternary composition on osteoblast and osteoblast-like proliferation, differentiation, and death in vitro. Acta Biomater. 2007;3:563–72.
36. Abou Neel EA, Mizoguchi T, Ito M, Bitar M, Salih V, Knowles JC. In vitro bioactivity and gene expression by cells cultured on titanium dioxide doped phosphate-based glasses. Biomaterials. 2007;28:2967–77.
37. Pietak AM, Reid JW, Stott MJ, Sayer M. Silicon substitution in the calcium phosphate bioceramics. Biomaterials. 2007;28: 4023–32.

38. Bohner M. Silicon substituted calcium phosphates–A critical view. Biomaterials. 2009;30:6403–6.
39. Ma S, Yang Y, Carnes DL, Kim K, Park S, Oh SH, Ong JL. Effect of dissolved calcium and phosphorous on osteoblast responses. J Oral Implantol. 2005;XXXI:61–7.
40. Ahmed I, Cronin PS, Abou Neel EA, Parson AJ, Knowles JC, Rudd CD. Retention of mechanical properties and cytocompatibility of a phosphate-based glass fiber/polylactic acid composite. J Biomed Mater Res B Appl Biomater. 2009;89:18–27.